Powder Technology 367 (2020) 183–191

Contents lists available at ScienceDirect

Powder Technology

journal homepage: www.elsevier.com/locate/powtec

Stretching the limits of dynamic and quasi-static flow testing on cohesive limestone powders

Hao Shi [a,*], Geoffroy Lumay [b], Stefan Luding [a]

[a] Multi-Scale Mechanics, TFE, ET, MESA+, University of Twente, PO Box 217, 7500 AE, Enschede, the Netherlands
[b] GRASP Laboratory, CESAM Research Unit, University of Liège, Belgium

ARTICLE INFO

Article history:
Received 5 September 2019
Received in revised form 12 March 2020
Accepted 15 March 2020
Available online 17 March 2020

Keywords:
Cohesion
Ring shear test
GranuHeap
GranuDrum
Bulk friction
Static-to-dynamic tests
Cohesive limestone powder

ABSTRACT

Powders are a special class of granular matter due to the important role of cohesive forces. Because the flow behavior of powders depends on both their flow states and confining stresses, it is difficult to measure/quantify with only one experiment. In this study, the most commonly used characterization tests that cover a wide range of states are compared: (static, free surface) angle of repose, the (quasi-static, confined) ring shear steady state angle of internal friction, and the (dynamic, free surface) rotating drum flow angle are considered for free flowing, moderately and strongly cohesive limestone powders.

The free flowing powder gives good agreement of angles among all different situations (devices), while the moderately and strongly cohesive powders behave more interestingly. Starting from the flow angle in the rotating drum and going slower, one can extrapolate to the limit of zero rotation rate, but then observes that the angle of repose measured from the static heap is considerably larger, possibly due to its special history. When we stretch the ring shear test to its lowest confining stress limit, the steady state angle of internal friction of the cohesive powder becomes comparable with the flow angle (at free surface) in the zero rotation rate limit of the rotating drum test, by defining an appropriate effective stress.

1. Introduction

Granular media are a collection of discrete solid particles interacting through dissipative contact forces; their natural discontinuity poses many challenges for both academia and industry in understanding their bulk behavior [1]. One of the challenges when dealing with granular media in processes is the characterization of these materials. While the characterization at the scale of the grains (size and shape distribution, …) is sometimes difficult, the macroscopic characterization (flow, packing fraction, tendency to segregate, …) is also tricky and a wide variety of tests are available [2].

Since decades, granular media have been subject to many fundamental studies, ranging from static to flowing conditions, from hard to soft particles, and from low to very high stresses. Micro-mechanical studies of granular materials give an essential understanding of their macro-scale behavior. For example, at *micro* or *meso* scale, the study by Radjai et al. [3] classifies the contacts into subnetworks of strong and weak contacts: the anisotropic shear stress of granular materials is primarily carried by the strong contacts. This method offers insight into the micro structure change from the contact origin but has its limitations for studying real life materials, e.g., limestone powders, especially the very fine ones which are strongly cohesive. The cohesion at micro scale can not be easily scaled up due to the complexity at *meso* scale [4,5,6], and there are still little focuses on the interesting behaviour of cohesive granular flow.

At macroscopic scale, from the perspective of granular flow, researchers have investigated different dynamic flow configurations like plane shear cells, Couette cells, silos, flows down inclined planes, or avalanches on piles and in rotating drums [7,8,9,10,11,12,13,14,15], where the granular materials are usually under very low or even free surface conditions. From the perspective of material characterization, researchers have developed various element tests in the lab to quantify the bulk responses of granular materials under specific stress/strain conditions. Element tests are (ideally homogeneous) macroscopic laboratory tests in which the force (stress) and/or displacement (strain) path are controlled. One of the most widely performed element tests in both industry and academia is the shear test in various designs [16,17,18,19,20,21,22,6], where a granular sample is sheared until failure is reached and the material starts to flow. The shear zone is predefined by the device design, and the shear failure is forced in a specific physical location. Another common element test is the uni-axial compression tester [23,24,25] where the lateral stress (λ-test) is more challenging but could be measured in a bi-axial shear box [26,27,28]. All these element tests are done in static to quasi-static flow regimes,

* Corresponding author.
E-mail addresses: h.shi-1@utwente.nl (H. Shi), geoffroy.lumay@uliege.be (G. Lumay), s.luding@utwente.nl (S. Luding).

https://doi.org/10.1016/j.powtec.2020.03.036

Table 1
Material parameters of the limestone samples. The initial bulk density represents bulk density from raw materials, as provided by the manufacturer.

Property		Unit	Eskal 300	Eskal15	Eskal150
Particle Size	d_{10}	μm	0.78	12	97
	d_{50}	μm	**2.22**	**19**	**138**
	d_{90}	μm	4.15	28	194
Span	$(d_{90}\text{-}d_{10})/d_{50}$	[−]	1.52	0.84	0.70
Particle density	ρ_p	kg/m^3	2853	2737	2761
Moisture content	w	%	0.9	0.9	0.9
Roundness	Ψ	[−]	0.75	0.48	0.88
Initial bulk density	ρ_0	kg/m^3	540	1110	1370

The bold numbers are the median particle size which is considered to be the average particle diameter by mass. These are the numbers referred to in the text multiple times.

with the stress applied usually above a few hundred pascals, while the granular flow tests mentioned above are normally carried out under more dynamic, and lower stress conditions.

In parallel to the classical shear cell test, different methods are commonly used to measure powder flow behavior: the angle of repose [29,30], the Hausner ratio [31,32], flow in rotating drums [33,34,35], flow through orifices [36], and powder rheometers with rotating blades inspired by liquid rheometers [37,38]. Different types of each test exist from the simple manual [39] to automatic versions [14,32].

Some of the flow tests are dynamic while others are static or quasi-static. Moreover, some tests are conducted with a free powder surface, whereas others are performed under confinement. Finally, both flow and stress fields are depending on the geometry of the tester. The link between different tests is mostly missing and represents a great challenge. Therefore, in this study, we explore the connection between two types of tests by stretching their limits: explore the dynamic rotating drum towards very low rotation rate, hence going to the quasi-static regime; and bring the quasi-static ring shear tests towards very low confining stresses, thus approaching the stress conditions in the dynamic drum test.

This study is structured as follows. Section 2 introduces the limestone materials; the description of the experimental devices and the test procedures are given in section 3. Section 4 is devoted to the discussion of experimental results and bridging between dynamic and quasi-static tests and covering a wide stress range. Conclusions and outlook are presented in section 5.

2. Material description and characterization

Limestone powder is a widely used powder in fields ranging from construction to automotive industries. In this work, eight grades of pre-sieved limestone powder under the commercial name Eskal (KSL Staubtechnik GmbH, Germany) are used. Eskal has been used as a reference powder for standard testing [6] and calibration of equipment in powder technology, for instance, shear testers [40,41], and optical sizing systems due to its favourable physical properties: high roundness, low porosity and an almost negligible sensitivity to humidity and temperature changes, which allows to avoid sample pretreatment.

Each grade of the Eskal series is milled and then sieved to ensure a certain particle size distribution. Three grades of Eskal are chosen specifically from the experience in a previous study [6]: fine/cohesive Eskal300 (d_{50} = 2.22 μm), slightly cohesive Eskal15 (d_{50} = 19 μm) and coarse/free-flowing Eskal150 (d_{50} = 138 μm). The details of their physical properties are summarized in Table 1.

The aspect ratio, shape and morphology of Eskal 150 and Eskal 300 are analyzed by means of Scanning Electron Microscope (SEM) imaging. Materials were sputtered with silver and investigated with a field emission instrument (Helios G4 CX, FEI Deutschland GmbH, Germany) with an EDX detector, applying an acceleration voltage of 5 kV and a working distance of 4 or 6 mm. Different magnifications between 185× and 15,000× were applied. Figs. 1 and 2 show the SEM images of Eskal150 and Eskal300, respectively. In Fig. 1, we see that all the Eskal150 primary particles have similar shapes (left) and rough surfaces (right), and every particle is clearly distinguished/separated from the others. In contrast, for Eskal300 in Fig. 2 (left), we observe some clusters of primary particles, and the size of clusters is typically around 50 to 100 μm, which is about 25 to 50 times the median particle size of Eskal300. When we zoom into a smaller scale, focusing on one single cluster as shown in Fig. 2 (right), we see even smaller fines (< 1 μm) sticking on the surface of primary particles. Moreover, the shapes of Eskal300 particles are more irregular than Eskal150 particles.

3. Experimental setup

In this study, we combine three experimental devices: GranuHeap (angle of repose), Schulze ring shear tester (steady state angle of internal friction), and GranuDrum (flow angle), to perform measurements in both static and dynamic regimes. The details of each setup are shown in Fig. 3 and will be explained in the following.

3.1. GranuHeap - static free surface

The angle of repose test has been widely used since 1943 in the particle and powder community. Al-Hashemi and Al-Amoudi presented a very wide review on different methods to obtain the angle of repose both experimentally and numerically [42]. The GranuHeap instrument [14] is an automated repose angle measurement device based on image processing and uses the principle of hollow cylinder method categorized in [42]. A powder heap is created on a cylindrical support to be

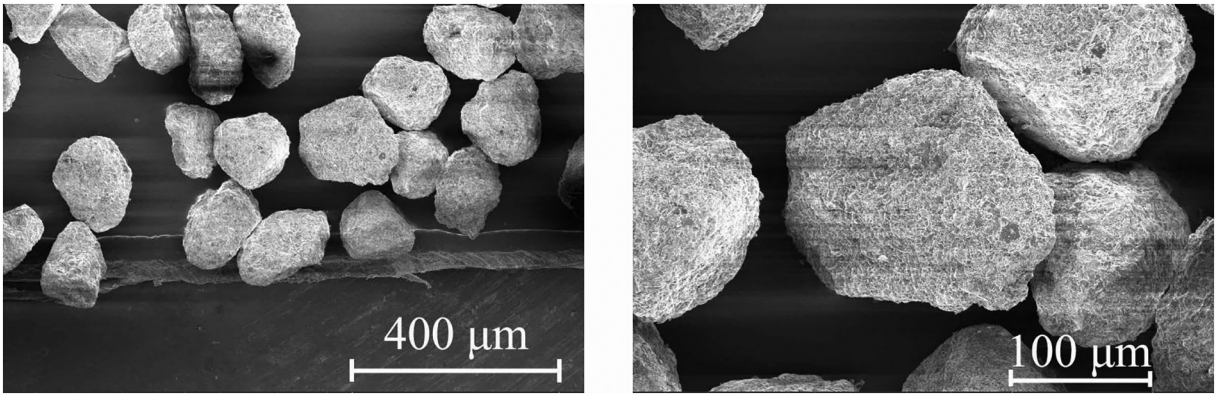

Fig. 1. SEM images of Eskal150 (d_{50} = 138 μm) in two different magnifications: 185× (left) and 502× (right).

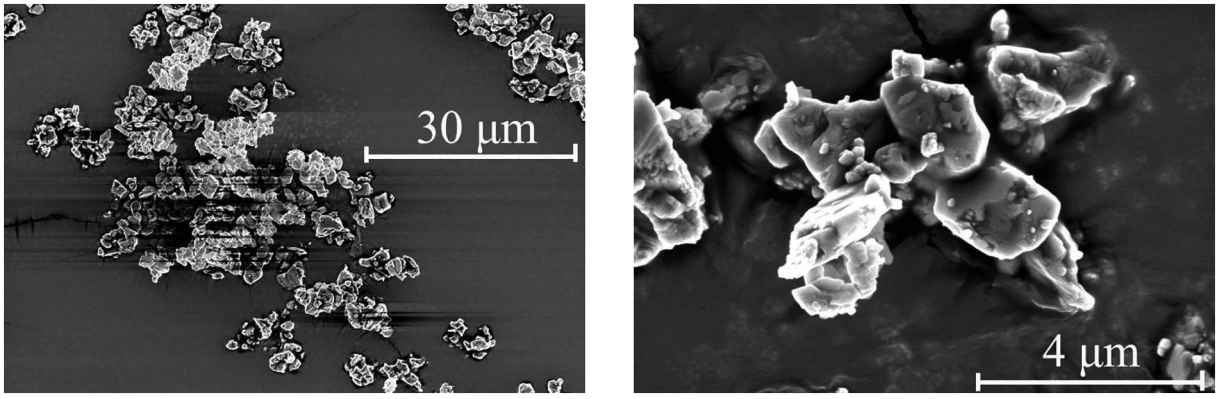

Fig. 2. SEM images of Eskal300 ($d_{50} = 2.2$ μm). Magnifications: 2500× (left) and 15,000× (right).

analyzed by image processing. The geometry of the measurement cell and a typical heap are presented in Fig. 3 (left). In order to obtain reproducible results, an initialization tube with an internal diameter equal to the circular support is installed on the support. After filling the initialization tube by hand with a fixed volume of powder (100 ml in the present study), the tube moves up at a constant speed of 5 mm/s. Thereby, the powder is flowing from the tube to form a heap on the cylindrical support, which is then evaluated by image analysis. A controlled rotation of the support allows obtaining different heap projections. In the present study, 16 images separated by a rotation angle of 11.25° were recorded. A custom image recognition algorithm determines the position of the powder/air interface. The angle of repose ϕ_{sta} refers to the angle of the isosceles triangle with the same projected surface as the powder heap. The isosceles triangle corresponds to the ideal heap shape. The lower the repose angle is, the better the powder flowability is [4]. A static cohesive index σ_{sta} can be also measured from the interface irregularities (not shown in the present study).

3.2. Schulze ring shear tester - RST-01 - quasi-static confined surface

Shear testers are used for powder characterization since decades. The Schulze rotational ring shear tester (1994) is one of the most widely used testers and it is semi-automated. The Schulze ring shear tester (RST-01) operates connected to a personal computer running a control software that allows the user to obtain, among other things, yield loci and wall yield loci. The ring-shaped (annular) bottom ring of the shear cell contains the bulk solid specimen. An annular-shaped lid is placed on top of the bulk solid specimen and it is fixed at a cross-beam (Fig. 3, middle). A normal force, F_N, is exerted on the cross-beam in the rotational axis of the shear cell and transmitted through the lid onto the specimen, i.e., a controlled normal stress is applied to the bulk solid. In order to allow small confining stress, the counterbalance force, F_A, acts in the centre of the cross-beam, created by counterweights and directed upwards, counteracting the gravity forces of the lid, the hanger and the cross-beam. Shearing of the sample is achieved by rotating the bottom ring with an angular velocity ω, whereas the lid and the cross-beam are prevented from rotation by two tie-rods connected to the cross-beam. Each of the tie-rods is fixed at a load beam, so that the forces, F_1 and F_2, acting on the tie-rods can be measured. The bottom of the shear cell and the lower side of the lid are rough in order to prevent sliding of the bulk solid on these two surfaces. Therefore, rotation of the bottom ring relative to the lid creates a shear deformation within the bulk solid. Through this shearing the bulk solid is deformed, and thus a shear stress τ develops, proportional to the forces on the tie-rods ($F_1 + F_2$). All the tests performed here follow the procedure as in the ASTM standard [43].

Typical confining stresses used in the shear cell tests are between 1 and 10 kPa. However, this is too high compared to the pressure range of free or nearly free surface. Thus, in order to explore the low confining stress regime, we employ the pre-shear normal stresses down to the device's lowest limit: 2, 1.5, 1.0, 0.8, 0.6, 0.4, 0.2 and 0.1 kPa. For cohesive Eskal300, we could apply the pre-shear normal stresses down to 0.1 kPa, whereas for free-flowing Eskal150, the minimum is at 0.2 kPa. And in order to achieve very low pre-shear normal stress in RST-01,

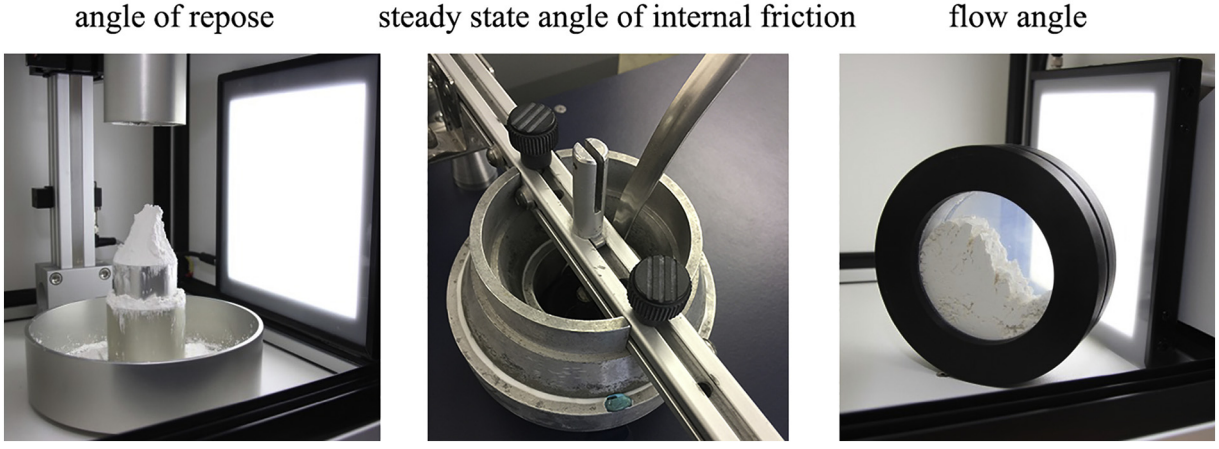

Fig. 3. Left: GranuHeap for measuring angle of repose; middle: the Schulze ring shear tester RST-01 for measuring steady state angle of internal friction; right: GranuDrum for measuring the flow angle.

we use a special shear cell lid made of PVC instead of aluminium, which has a lower self weight of the lid and allows to apply very low stress. However, at the lowest stresses the pre-consolidation becomes questionable and the output is not representative. For each pre-shear normal stress, we performed three runs, with every time a fresh sample, in order to investigate repeatability. In all tests presented here, the shear velocity is kept constant (1 mm/min) as default to ensure that the shearing is within the quasi-static regime. A typical testing procedure is as follows: first vertically compress the sample to the predefined pre-shear normal stress value, e.g. 1 kPa and deploy shear, the control software will wait until the shear stress is almost constant then stop the shearing. Then the first pre-shear point is obtained. The normal stress is kept at pre-shear and the lid will rotate backwards to reach a zero shear stress state, then the normal stress will reduce to the first shear point, e.g. 0.4 kPa and continue shearing. After a peak failure in the shear stress is detected, the first shear cycle is finished and thus the first shear point is obtained. The software/program will continue this pre-shear then shear procedure until all the shear points are measured. A more detailed explanation of different procedures are given in [6,21] and will not be further addressed here for the sake of brevity.

3.3. GranuDrum - dynamic free surface

The GranuDrum instrument [14] is an automated powder flowability measurement technique based on the rotating drum geometry, which characterizes materials in the dynamic flowing regime with a free surface. A horizontal cylinder with vertical glass side walls (called drum) is half filled with the sample of powder. For the present study, the drum rotates around its horizontal axis of symmetry at rotation speeds from 1 RPM to 10 RPM (increase sequence) and we do not measure the flow during the rotation speed decrease sequence, which more relevant to the hysteresis of the powder flow. A CCD camera takes snapshots (50 images separated by 0.5 s) at each angular velocity (see Fig. 3 right). The air/powder interface is detected on each snapshot with an edge detection algorithm. Afterward, the average interface position and the fluctuations around this average position are computed. Then, for each rotation speed, the dynamic friction (flow) angle ϕ_{dyn} is measured at the center of the average interface position. A dynamic cohesive index σ_{dyn} can be also measured from the interface fluctuations (not shown in the present study).

3.4. Interpretation of the results

In order to compare the confined surface ring shear test to the free surface GranuHeap and GranuDrum, we proposed a simple method to estimate the (effective) confining stress on flowing powders in both GranuHeap and GranuDrum tests by two principles: single particle layer h_0 and effective flowing depth of the rotating drum h. The first one represents the effective pressure induced by a single layer of primary particles in the static GranuHeap test. In the static situation, one expects the relevant depth close to the free surface to be of the same order as the particle diameter.

The effective flowing depth is more appropriate for the case of the rotating drum and given by the ratio between the actual flowing depth h and the radius r of the drum $h_{eff} = h/r$. The flowing depth of non-cohesive granular materials in a rotating drum depends on the rotation speed and on the ratio between the drum diameter and the grain diameter [44]. For cohesive powders, the flowing depth increases with the cohesiveness [45], the powder particles will form agglomerates/aggregates during the flow/movement, but those agglomerates/aggregates are not fully stable, they might break and reform again. It is almost impossible to get an accurate measurement of the depth of the flowing layer for our most cohesive Eskal300. Therefore, instead of giving an estimation of the flowing depth, we use a depth range: 1% to 100% of the drum radius, which covers mostly the possible depths of cohesive powder flows in a rotating drum [45]. Then, the effective confining stresses are evaluated at different depths h inside the powder bed considering the hydrostatic pressure $\sigma = \rho_{bulk} g h$, where ρ_{bulk} is the powder bulk density and g is the gravitational acceleration.

4. Results and discussion

4.1. Static granular heap

Fig. 4 shows typical heaps obtained with Eskal150 (left) Eskal15 (middle) and Eskal300 (right). The heap obtained with free flowing Eskal150 has an almost conical shape with a rather low angle of repose ($\phi_{sta} = 33.0 \pm 0.1°$). The cohesive Eskal300 powder forms a strongly irregular heap with a high static friction (repose) angle ($\phi_{sta} = 69.1 \pm 1.9°$) due to the influence of cohesion between particles. The heap obtained with Eskal15 has a slightly irregular conical shape and lies between the angles of repose of Eskal150 and 300 ($\phi_{sta} = 52.6 \pm 1.4°$). It has been reported that even for one measurement method, there are still difficulties in the repeatability and reproducibility, due to human/operator influences inside a single lab or at different labs [42]. In the current study, the repose angle measurement of each Eskal powder has been repeated four times with fresh samples to obtain a representative mean value with the rather good repeatability (standard deviations: 2.7% for cohesive Eskal300, 2.6% for moderately cohesive Eskal15 and 0.3% for free flowing Eskal150). This includes that the stably formed heap in each single measurement was rotated slowly to take 16 pictures at different viewing angles from the side of the heap and then averaged to obtain the final value.

Fig. 4. Typical heaps obtained with Eskal150, Eskal15 and Eskal300.

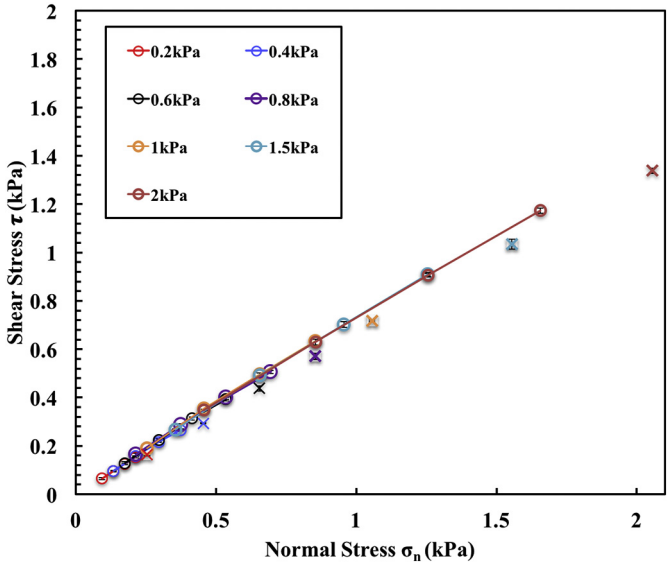

Fig. 5. Yield locus (shear stress versus normal stress) of Eskal150 ($d_{50} = 138$ μm) using RST-01. The pre-shear normal stress is kept between 0.2 and 2 kPa. Different colours indicate different pre-shear normal stresses. Points with and without lines are shear and pre-shear points, respectively. Lines are only guides to the eye.

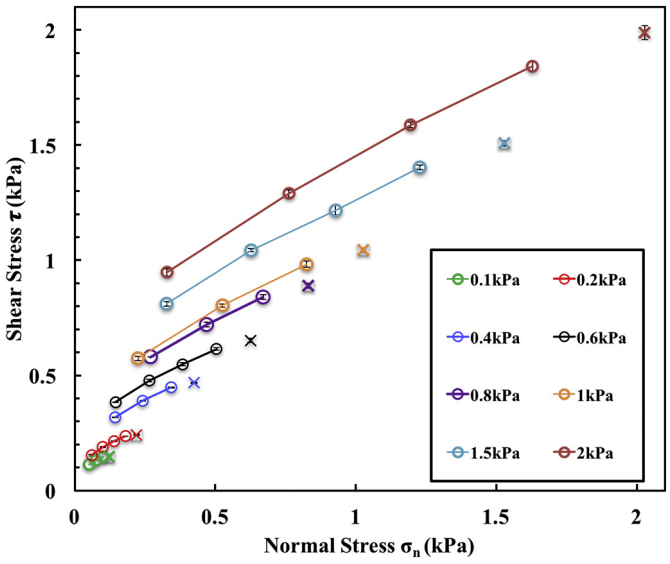

Fig. 6. Yield locus (shear stress versus normal stress) of Eskal300 ($d_{50} = 2.2$ μm) using RST-01. The pre-shear normal stress (*x* symbols) varied between 0.1 and 2 kPa, as given by different colours. Points with lines are shear data and lines are only guides to the eye. Note that this is only a zoom into the data range ≤ 2 kPa pre-shear normal stress level, more data can be found in [6,46].

4.2. Quasi-static ring shear tester

In the low confining (normal) stress regime, we first look at the yield loci at different pre-shear stresses (0.2 to 2 kPa) for Eskal150 ($d_{50} = 138$ μm) in Fig. 5 with different pre-shear stresses indicated by different colours. Each yield locus is measured with three fresh samples to acquire the standard deviations. With increase in pre-shear normal stress, all the yield loci collapse on a single curve. This is expected for free flowing powder, where the flow behaviour is not sensitive to the pre-shear confining stress. The pre-shear points stay consistently lower than the corresponding yield loci, with relative difference between the pre-shear points and yield loci increasing with the pre-shear normal stress. Both pre-shear and shear data show very good repeatability with maximum standard deviations around symbol size. We only manage to measure representative yield loci of Eskal150 down to 0.2 kPa pre-shear normal stress, while the data measured at lower stress levels are not reliable. Note that we have previously measured the yield loci at higher stress levels (see Ref. [6, 46]). For the sake of brevity, the data are not shown here, since they follow the trend of low stress levels. However, these data will also be included in the Fig. 9 below.

For the cohesive Eskal300 ($d_{50} = 2.2$ μm), we measured the yield loci in the normal stress range between 0.1 and 2 kPa, and the data are shown in Fig. 6. Unlike the free flowing Eskal150, the yield loci of Eskal300 move upwards with the increase of the pre-shear normal stress, which indicates the cohesive Eskal300 is sensitive to the pre-shear normal stress. The yield loci of Eskal300 show a convex curvature as clearly visible from the guide lines, as studied in detail in Ref. [46]. Similar to the case of Eskal150, the yield loci of Eskal300 show very good repeatability with maximum standard deviations around symbol size. Furthermore, we have also included the steady state angle of internal friction of moderate cohesive Eskal15 at three pre-shear stress levels: 5, 20 and 35 kPa (data only shown in Fig. 9) from our previous study [6] for the sake of completeness.

Four angles could be obtained from Fig. 6: (1) the effective angle of internal friction (from Mohr circle), (2) the angle of internal friction (from linearized yield loci) and (3) steady state angle of internal friction (from pre-shear points) [6] and (4) the unconfined angle of internal friction [46]. In the current study, we only use the latter (3) instead of the linearized (2) for further comparisons. For the yield loci of Eskal300 at various pre-shear normal stress, we have also used the non-linear Warren-Spring model [46] to obtain (4) the unconfined angle of internal friction (slope of this non-linear yield locus at zero confining stress): $\phi = 57.6°$, which is substantially lower than $\phi_{sta} = 69.1°$ of Eskal300 obtained from heap measurements, see Sec. 4.1.

4.3. Unifying the static and the dynamic states

Following the same principle as in Fig. 4 with heaps, Fig. 7 shows the typical flowing patterns obtained in the rotating drum with Eskal150 (left), Eskal15 (middle) and Eskal300 (right). The free flowing Eskal150 shows a very smooth free surface with a slightly concave shape, while the cohesive Eskal300 gives a much rougher free surface with some clumps due to cohesion. For slightly cohesive powder Eskal15, the result lays between Eskal150 and Eskal300 and the surface of Eskal15 powder is much smoother than Eskal300 with less clumps.

The flow angles of our three limestone powders at different rotation speeds Ω are measured with the GranuDrum and plotted in Fig. 8. With increasing Ω, the flowing angle increases for the free flowing Eskal150 and decreases for the cohesive Eskal300. This behavior is also commonly seen for other powders [14]. The increase with rotation speed for non-cohesive granular materials is due to the inertial effect, whereas the decrease for cohesive powders is due to stronger aeration at higher rotation speeds. A linear regression allows us to extrapolate to the angle at 0 rpm and we obtain $\phi_{dyn} = 32°$ for non-cohesive Eskal150, $\phi_{dyn} = 40°$ for slightly cohesive Eskal15 and $\phi_{dyn} = 62°$ for cohesive Eskal300. In addition, we also plotted in Fig. 8 the three angles of repose measured with the GranuHeap at zero rotation speed for comparison. For the free flowing Eskal150, the angle of repose measured from GranuHeap is comparable to the extrapolated flow angle at 0 rpm. However, for the cohesive powders Eskal15 and Eskal300, the angles of repose measured from the heaps, ϕ_{sta}, are considerably higher than the angle extrapolated from the GranuDrum data. This difference can be explained by the existence of two angles measured respectively before and after the slope instability (avalanches), which are named upper and lower angle [47]. The angle of repose measured in Sec. 4.1 represents the highest stable angles that Eskal300 and Eskal15 could ever reach (upper limit) while the flow angles vary between the upper and lower angles, consequently showing lower averages. Some previous studies

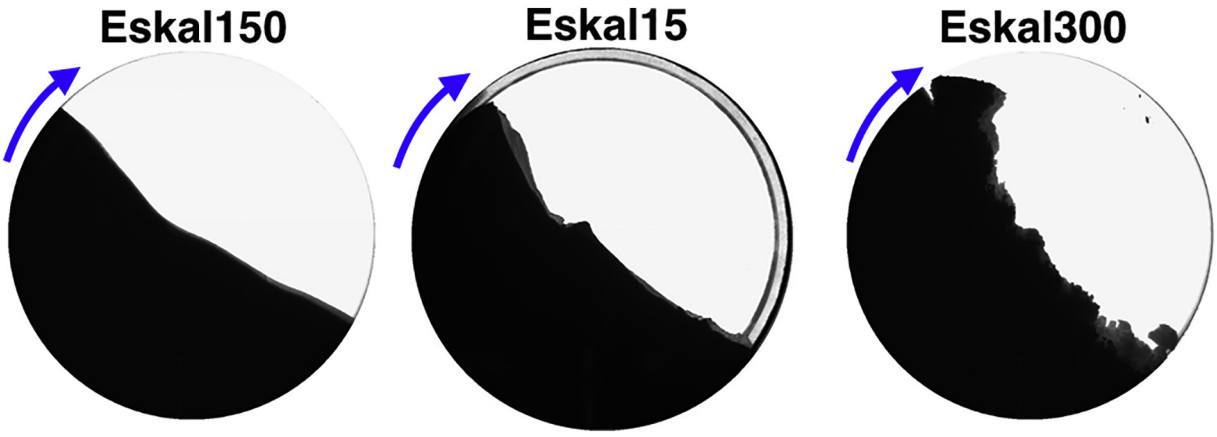

Fig. 7. Snapshots of typical flow patterns inside the rotating drum with Eskal150, Eskal15 and Eskal300.

[48,49,50] revealed several influencing factors of using the hollow cylinder preparation method, establishing a different history for the powder: stratification, interface friction angle (which is the friction angle between the base and the granular material), lifting velocity, cylinder size, base roughness, granular material mass and height of the material in the cylinder. As the lifting velocity, material mass and material height increase, the angle of repose decreases. However, when the roughness of the base increases, the angle of repose also increases. This could possibly explain the higher values we measured here as our lifting velocity (5 mm/s) and material mass (height control with low bulk density) are both low. If we increase the lifting velocity or the initial filling mass, the measured angle of repose is expected lower. However, our main goal here is to reach the static free surface limit without varying the standard testing protocol, therefore we keep the measurement conditions as they are.

Note that different PSDs could lead to the changes of powder flowability. For cohesive Eskal300, the size range is between 1 and 10 μm, thus we do not expect that a low energy input (zero to very low confining stress) will lead to much attrition. Instead, the agglomeration due to centrifugal forces and breakage due to impacts at high rotation speed could lead to significant change in the angles. For moderately cohesive Eskal15, the median particle size is almost 10 times larger than that of Eskal300, therefore the expected attrition/agglomeration effects should also be negligible. Moreover, here we focus on the steady state friction which is the angle that does not vary with time or further deformation. In this study, we try to avoid going to too high rotation speeds as our focus is the quasi-static limit state. For free flowing Eskal150, the steady state angle of internal friction stays almost constant when the pre-shear normal stress is low ($\sigma_{pre} < 3$ kPa) but decreases slightly at larger confining stresses ($\sigma_{pre} > 3$ kPa). Therefore, we speculate there might be some changes of the PSD at high confining stress levels.

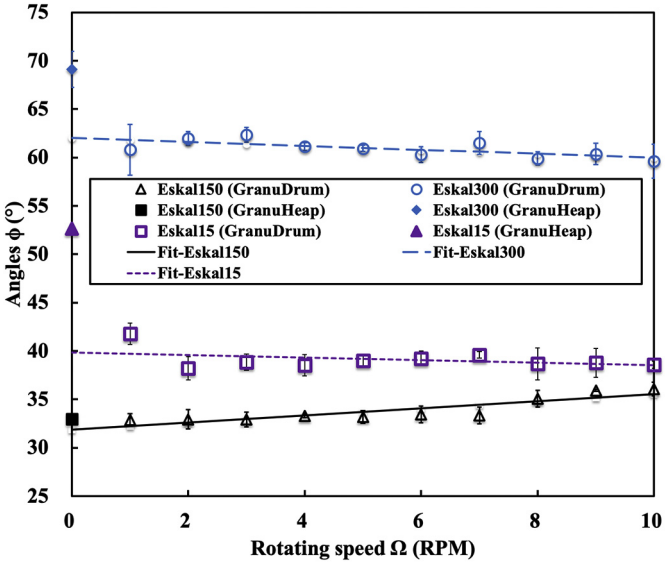

Fig. 8. Angle of repose measured with the GranuHeap (plain symbols) and the flow angles for different rotation speeds measured with the GranuDrum (open symbols). A linear regression allows to extrapolate the angle at 0 rpm from GranuDrum data with $\phi = \phi_{\Omega 0} + \phi_{\Omega 1}\Omega$, with $\phi_{\Omega 0} = 32\,^\circ$, $40\,^\circ$, 62° and $\phi_{\Omega 1} = 0.37, -0.13, -0.20$ for Eskal150, Eskal15 and Eskal300, respectively.

4.4. From small to large confining stress

After confirming the repeatability of each test, we come back to the main focus of this study: linking different flow regimes, not only from dynamic to static, but also from moderate to low and almost no confining stress. Our first step is to explore the quasi-static flow regime and extrapolate the steady state angle of internal friction towards zero confining stress, which is more relevant to a free surface flow. The second step is to determine the values of effective confining stress for both (static) GranuHeap and (dynamic) GranuDrum. Results can then be presented in a unique comprehensive plot showing the dependence of the friction angles ϕ on the confining stress σ for three tests and three materials.

In Fig. 9, the steady state angles of internal friction measured by the Schulze ring shear tester are plotted against the confining stress for the three selected Eskal powders. The confining stress axis is shown in logarithmic scale in order to represent better the low stress range. We have fitted Eskal150 data using a linear regression and the Eskal300 and 15 data using a logarithmic one, all extended towards the very low stress regime. Note that here we have also included the data at larger pre-shear stresses ($\sigma > 2$ kPa) from the previous studies [6,46] for the sake of completeness.

For the free flowing Eskal150, the linear regression in the low confining stress regime ($\sigma \leq 2$ kPa) is almost constant. This behaviour is mainly dominated by the surface properties of the primary particles, e.g., shape, roughness, and thus not much influenced by the confining stress. On the other hand, if the confining stress becomes larger ($\sigma > 2$ kPa), the fitted line decreases slightly with the confining stress, e.g., particles are rearranged to reduce the porosity or particles are more compressed towards each other to form contact flattening, and thus reduce the effect of particle surface irregularities. When we compare the Schulze ring shear tester data to the other two testers, for Eskal150, both angle of repose ϕ_{sta} (black arrow on angles axis) and flow angle ϕ_{dyn} at 0 rpm

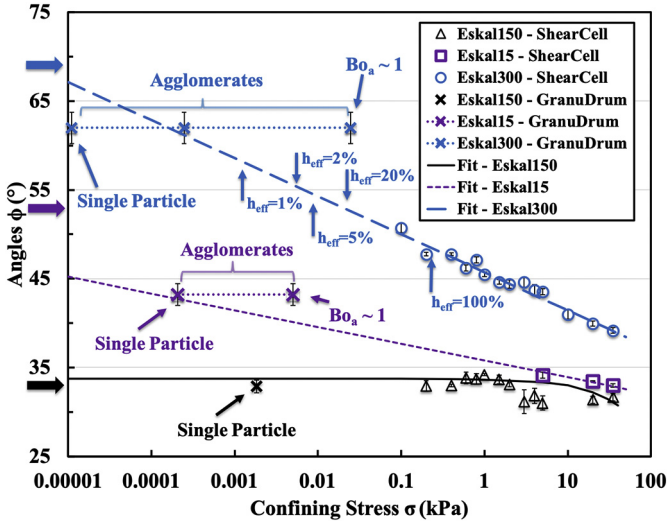

Fig. 9. Angles, ϕ, from different types of tests as a function of confining stress, σ, for Eskal150 (138 μm), Eskal15 (19 μm) and Eskal300 (2.2 μm) in semi-log scale. The confining stresses refer to the normal stress at pre-shear in the ring shear test, and the estimated stresses in the other two tests (see main text). Lines are the fitting to the shear test data: black linear regression line, $\phi = \phi_0(1 - \sigma/\sigma_\phi)$, with the limit ($\sigma \to 0$) angle $\phi_0 = 33.73°$ and characteristic stress $\sigma_\phi = 452$ kPa for Eskal150; dashed purple line, $\phi = \phi_1 - \Delta\phi \log(\sigma/\sigma_1)$, with $\phi_1 = 35.78°$, $\Delta\phi = 0.82°$ and $\sigma_1 = 1$ kPa for Eskal15; dashed blue line, $\phi = \phi_1 - \Delta\phi \log(\sigma/\sigma_1)$, with $\phi_1 = 45.85°$, $\Delta\phi = 1.86°$ and $\sigma_1 = 1$ kPa for Eskal300. Thick arrows on the angle axis indicate the measured angles of repose of three powders. Agglomerate refers to the clumps formed/destroyed due to the cohesiveness among powder particles. The flow angles of cohesive Eskal15 and 300 (due to agglomerates) are given as a range of effective confining stresses estimated between single particle layer and $Bo_a \sim 1$. The effective flowing depth in the rotating drum, $h_{eff} = h/r$ is also given as arrows between 1 and 100% for the strongly cohesive Eskal300. (For interpretation of the references to colour in this figure legend, the reader is referred to the web version of this article.)

(black cross) match well with the prediction (solid black fitting line) from the Schulze ring shear tester data, because this material is free flowing and insensitive to the confining stress in the low pressure range of interest.

For the cohesive Eskal300, a good fit is obtained by a logarithmic decay with stress.[1] This decreasing trend with confining stress is expected as powders normally flow better in the larger confining stress regime. The reason is that larger confining stress leads to larger rearrangements, plastic deformations and possibly contact flattening. This reduces not only the influences from surface roughness and geometrical interlocking, but also makes cohesion less important, and thus results in a reduction of flow resistance. We also tested this logarithmic decay using another slightly cohesive Eskal15 powder, for which the ring shear test data are taken from our previous study [6]. Although the shear test measurement points are few compared to the strongly cohesive Eskal300, the proposed decay looks plausible, but more data should be collected in future, and more advanced non-linear models [46] should be applied.

4.5. What about the effective stress scale?

From all the available data, we compare the steady state friction angle from the shear tester in Fig. 9, with the static and dynamic angles from the other two devices. Note that among all results that one obtains from shear testers for cohesive powders, the effective angle of internal friction is the maximal, the linearized yield angle of internal friction is the minimal, while the steady state angle of internal friction is intermediate. At the same time, the static angle of repose is a maximum, while the dynamic friction angle is an intermediate too.

For comparison of the different experiments, it is necessary to estimate the effective (confining and/or cohesive) stresses in GranuDrum and GranuHeap. For this, one could assume a certain depth h inside the powder bed to set the relevant hydro-static pressure $\sigma = \rho_{bulk} g h$, where ρ_{bulk} is the powder bulk density and g is gravitational acceleration. As first idea, using the size (and thus the weight) of a single particle as the relevant stress scale – plausible only if there are no agglomerates expected – for free flowing Eskal150, we estimate $\sigma_1^{150} \approx 0.0018$ kPa, using $h \approx d_{50} = 138$ μm with the bulk density $\rho_{bulk} = 1354$ kg/m^3. Similar estimates for Eskal15 ($h = 19$ μm, $\rho_{bulk} = 1110$ kg/m^3) and Eskal300 ($h = 2$ μm, $\rho_{bulk} = 501$ kg/m^3) result in very low $\sigma_1^{15} \approx 0.00021$ kPa and $\sigma_1^{300} \approx 0.00001$ kPa, respectively. Alternatively, assuming clusters/agglomerates to prevail in Eskal300 ($h = d_a \approx 50$ μm, as a mere guess) would result in $\sigma_a^{300} \approx 0.00025$ kPa, i.e., accidentally very similar to σ_1^{15}.

Another idea is to use the principle of an effective flowing depth h_{eff} (see Sec. 3 for details) to evaluate different stress levels. The estimated confining stresses in the rotating drum are indicated by arrows along the trend-line in Fig. 9. A level of 100% corresponds to the stress at the bottom of a half-filled drum with radius $r = 4.8$ cm, i.e., in each rotation, some of the powder experiences stress levels comparable to the lower end of the shear tester confining stresses. The flowing layer is typically much shallower, e.g., about 20% of the drum radius, i.e., $h \approx 10$ mm, results in a stress level of about $\sigma \approx 0.05$ kPa. For cohesionless particles, the flowing zone (shear band) is often assumed as being order of 10 particle diameters thick, whereas the flow in cohesive powders is sometimes more like a snow-ball rolling down an inclined slope, a situation for which the flow angle measurement becomes questionable.

The third idea to predict effective stress levels is using the macroscopic cohesion (cohesive strength) C to estimate cohesive forces: $f_c \approx Cd^2$, and gravitational force $f_g = \rho_p g(\pi/6)d^3$, to obtain a Bond number $Bo_g = f_c/f_g = 6C/(\pi\rho_p g d) = d_C/d$, with cohesive length scale d_C. This turns out to be $Bo_g^{300} \approx 3000$ and $Bo_g^{15} \approx 30$, for which the (estimated) cohesive strengths $C^{300} = 0.08$ kPa and $C^{15} = 0.008$ kPa were used (based on an assumed confining stress of $h \approx 0.05$ m material weight, i.e., $\sigma \approx 0.25$ kPa, as relevant in the GranuDrum setup during every rotation, and in the GranuHeap during preparation). Inverted, this argument transforms into an estimated cluster/agglomerate size of $d_a \approx d_C$, assuming that typical clusters live at $Bo_a \sim 1$, resulting in $d_a^{300} \approx 5$ mm and $d_a^{15} \approx 0.5$ mm. Plugging those estimated agglomerate sizes back into the pressure estimate yields $\sigma_a^{300} = 0.025$ kPa and $\sigma_a^{15} = 0.005$ kPa.

5. Conclusion and outlook

In this study, we have examined the flow behaviour of three non-cohesive (Eskal150, $d_{50} = 138$ μm), moderately cohesive (Eskal15, $d_{50} = 19$ μm) and strongly cohesive (Eskal300, $d_{50} = 2.2$ μm) limestone powders in three characterization tests: GranuHeap (static angle of repose), Schulze ring shear test (steady state angle of internal friction) and GranuDrum (dynamic flow angle). Tests at various confining stresses are performed in the Schulze ring shear tester and are extrapolated towards almost zero confining stress with empirical laws. This offers the possibility to link to other tests involving low stress states at free surfaces. To our knowledge, there is no similar study done before, although all those tests have been used in the powder technology community for a very long time.

The angle of repose of free flowing Eskal150 measured with GranuHeap is much lower than the angle of repose of Eskal300, with the angle of Eskal15 in between, which confirms that cohesion correlates with higher angles (shear resistance) for the same material, but smaller size.

The flow angle of Eskal150 measured with GranuDrum increases at large rotation speeds, while a weak decrease is observed for Eskal300

[1] Note that this fit diverges towards zero confining stress, where it thus must not be used.

but no clear trend for Eskal15. This is because faster motion of free flowing and cohesive powders is expected to be dominated by inertial effects and aeration, respectively. The extrapolation of the flow angle of Eskal150 to 0 rpm agrees well with the measured angle of repose. However, the extrapolations of the flow angle of Eskal15 and Eskal300 to 0 rpm are significantly lower than the angles of repose, i.e., the highest stable angle, whereas the flow angles are the average between the angles of repose and the angles after an avalanche.

The steady state angle of internal friction obtained by quasi-static ring shear tests is found to be a function of both confining stress and material. The data of free flowing Eskal150 are fitted well by a linear regression, whereas the cohesive Eskal300 is well described by a logarithmic decay. Such empirical laws allow us to predict angles of very low confining stresses that are comparable with the other two types of test. For free flowing Eskal150, all three tests agree very well with each other. For the cohesive Eskal300, the estimation of the effective confining stress is very difficult for the free surface tests. Three possible ways of estimating the effective stress are proposed, which indicate a range of possible active, effective mechanisms inside the flowing powder bed. Furthermore, the few available results of the slightly cohesive Eskal15 are also described well with a similar but weaker logarithmic decay with confining stress.

In summary, our method opens new perspectives in the field of powder characterization and for measurement interpretation. Cohesive powders in industrial process lines with small to moderate stresses often suffer from unusually large bulk friction, cohesion, and thus flow problems. The empirical logarithmic stress dependence of the steady state angle of internal friction allows to close some gaps, where measurements are difficult.

In future, the applicability of the proposed empirical laws and stress-estimates should be further checked by including other materials and alternative testing techniques. Also a more detailed study on the effective flowing layer depth in a rotating drum for cohesive powders is needed as well as inside views into both heap and shear cell to understand the remaining differences in the results.

CRediT author statement

Hao Shi: Conceptualization, Methodology, Experimental Data Collection, Draft Preparation, Writing.

Geoffroy Lumay: Experimental Data Collection, Methodology, Draft Preparation, Writing.

Stefan Luding: Supervision, Reviewing and Editing.

Declaration of Competing Interest

The authors declare that there is no conflict of interest.

Acknowledgement

We would like to thank for the financial support through the “T-MAPPP” project of the European-Union-Funded Marie Skłodowska-Curie Initial Training Network FP7 (ITN607453), in which the Schulze ring shear measurements were carried out. GranuDrum and GranuHeap measurements were conducted in the framework of the “PowderReg” project (017-4-08-06), funded by the European programme Interreg VA GR within the priority axis 4 “Strengthen the competitiveness and the attractiveness of the Grande Région / Großregion”. The help from R. Cabiscol on making the SEM images and shear test experiments is also greatly acknowledged.

Appendix A. Supplementary data

Supplementary data to this article can be found online at https://doi.org/10.4121/uuid:bbcb782b-5e89-4cb9-8b8e-d4fe42c26de1.

References

[1] H.M. Jaeger, S.R. Nagel, R.P. Behringer, Granular solids, liquids, and gases, Rev. Mod. Phys. 68 (1996) 1259–1273.
[2] J. Schwedes, Review on testers for measuring flow properties of bulk solids, Granul. Matter 5 (2003) 1–43.
[3] F. Radjai, D.E. Wolf, M. Jean, J. Moreau, Bimodal character of stress transmission in granular packings, Phys. Rev. Lett. 80 (1998)61+.
[4] J. Tomas, Adhesion of ultrafine particles–a micromechanical approach, Chem. Eng. Sci. 62 (2007) 1997–2010.
[5] N. Berger, E. Azéma, J.F. Douce, F. Radjai, Scaling behaviour of cohesive granular flows, EPL (Europhys. Lett.) 112 (2016) 64004.
[6] H. Shi, R. Mohanty, S. Chakravarty, R. Cabiscol, M. Morgeneyer, H. Zetzener, J.Y. Ooi, A. Kwade, S. Luding, V. Magnanimo, Effect of particle size and cohesion on powder yielding and flow, KONA Powder Part. J. 35 (2018) 226–250.
[7] G.D.R. MiDi, On dense granular flows, Eur. Phys. J. E 14 (2004) 341–365.
[8] P. Jop, Y. Forterre, O. Pouliquen, A constitutive law for dense granular flows, Nature 441 (2006) 727–730.
[9] O. Pouliquen, C. Cassar, P. Jop, Y. Forterre, M. Nicolas, Flow of dense granular material: towards simple constitutive laws, J. Stat. Mech. 2006 (2006) P07020.
[10] G. Lumay, N. Vandewalle, C. Bodson, L. Delattre, O. Gerasimov, Linking compaction dynamics to the flow properties of powders, Appl. Phys. Lett. 89 (2006), 093505.
[11] Y. Forterre, O. Pouliquen, Flows of dense granular media, Annu. Rev. Fluid Mech. 40 (2008) 1–24.
[12] P. Schall, M. van Hecke, Shear bands in matter with granularity, Annu. Rev. Fluid Mech. 42 (2010) 67–88.
[13] G. Lumay, N. Vandewalle, Flow of magnetized grains in a rotating drum, Phys. Rev. E 82 (2010), 040301.
[14] G. Lumay, F. Boschini, K. Traina, S. Bontempi, J.C. Remy, R. Cloots, N. Vandewalle, Measuring the flowing properties of powders and grains, Powder Technol. 224 (2012) 19–27.
[15] A. Jarray, V. Magnanimo, S. Luding, Wet granular flow control through liquid induced cohesion, Powder Technol. 341 (2019) 126–139.
[16] A. Casagrande, The determination of the pre-consolidation load and its practical significance, Proceedings of the International Conference on Soil Mechanics and Foundation Engineering, volume 3, Harvard University Cambridge 1936, pp. 60–64.
[17] A.W. Jenike, Storage and flow of solids, bulletin no. 123, Bul. Univ. Utah 53 (1964).
[18] J. Schwedes, Vergleichende Betrachtungen zum Einsatz von Schergeräten zur Messung von Schüttguteigenschaften, Proc. PARTEC, Nürnberg 1979, pp. 278–300.
[19] D. Schulze, Entwicklung und Anwendung eines neuartigen Ringschergerätes, Aufbereitungs-Technik 35 (1994) 524–535.
[20] S. Shibuya, T. Mitachi, S. Tamate, Interpretation of direct shear box testing of sands as quasi-simple shear, Geotechnique 47 (1997) 769–790.
[21] D. Schulze, Powders and Bulk Solids: Behavior, Characterization, Storage and Flow, Springer, 2008.
[22] U. Zafar, C. Hare, G. Calvert, M. Ghadiri, R. Girimonte, B. Formisani, M.A.S. Quintanilla, J.M. Valverde, Comparison of cohesive powder flowability measured by schulze shear cell, raining bed method, Sevilla powder tester and new ball indentation method, Powder Technol. 286 (2015) 807–816.
[23] A. Russell, P. Müller, H. Shi, J. Tomas, Influences of loading rate and preloading on the mechanical properties of dry elasto-plastic granules under compression, AICHE J. 60 (2014) 4037–4050.
[24] S.C. Thakur, H. Ahmadian, J. Sun, J.Y. Ooi, An experimental and numerical study of packing, compression, and caking behaviour of detergent powders, Particuology 12 (2014) 2–12.
[25] O.I. Imole, M. Paulick, V. Magnanimo, M. Morgeneyer, B.E. Montes, M. Ramaioli, A. Kwade, S. Luding, Slow stress relaxation behavior of cohesive powders, Powder Technol. 293 (2016) 82–93.
[26] M. Morgeneyer, L. Brendel, Z. Farkas, D. Kadau, D.E. Wolf, J. Schwedes, Can one make a powder forget its history? Proceedings of the 4th International Conference for Conveying and Handling of Particulate Solids, Budapest 2003, pp. 12–118.
[27] M. Morgeneyer, J. Schwedes, Investigation of powder properties using alternating strain paths, Task Quart. 7 (2003) 571–578.
[28] H. Feise, J. Schwedes, Investigation of the behaviour of cohesive powder in the biaxial tester, KONA Powder Part. J. 13 (1995) 99–104.
[29] Y.C. Zhou, B.H. Xu, A.B. Yu, P. Zulli, An experimental and numerical study of the angle of repose of coarse spheres, Powder Technol. 125 (2002) 45–54.
[30] K. Ileleji, B. Zhou, The angle of repose of bulk corn stover particles, Powder Technol. 187 (2008) 110–118.
[31] R. Grey, J. Beddow, On the Hausner ratio and its relationship to some properties of metal powders, Powder Technol. 2 (1969) 323–326.
[32] K. Traina, R. Cloots, S. Bontempi, G. Lumay, N. Vandewalle, F. Boschini, Flow abilities of powders and granular materials evidenced from dynamical tap density measurement, Powder Technol. 235 (2013) 842–852.
[33] X.Y. Liu, E. Specht, J. Mellmann, Experimental study of the lower and upper angles of repose of granular materials in rotating drums, Powder Technol. 154 (2005) 125–131.
[34] S.L. Pirard, G. Lumay, N. Vandewalle, J.-P. Pirard, Motion of carbon nanotubes in a rotating drum: the dynamic angle of repose and a bed behavior diagram, Chem. Eng. J. 146 (2009) 143–147.
[35] V.R. Nalluri, M. Kuentz, Flowability characterisation of drug–excipient blends using a novel powder avalanching method, Eur. J. Pharm. Biopharm. 74 (2010) 388–396.
[36] H. Ahn, Z. Başaranoğlu, M. Ylmaz, A. Buğutekin, M.Z. Gül, Experimental investigation of granular flow through an orifice, Powder Technol. 186 (2008) 65–71.

[37] R. Freeman, Measuring the flow properties of consolidated, conditioned and aerated powders - a comparative study using a powder rheometer and a rotational shear cell, Powder Technol. 174 (2007) 25–33.
[38] L.F. Madariaga, P. Marchal, C. Castel, E. Favre, L. Choplin, Characterization of impregnated particles via powder rheology, Powder Technol. 196 (2009) 222–228.
[39] E. P. Commission, E. D. for the Quality of Medicines & Healthcare, European pharmacopoeia 7.0, Chapter 2.9.36 : Powder flow, volume 1 Council of Europe, 2010.
[40] H.J. Feise, A review of induced anisotropy and steady-state flow in powders, Powder Technol. 98 (1998) 191–200.
[41] H. Zetzener, J. Schwedes, Relaxation and creep of dry bulk solids, Part. Part. Syst. Charact. 19 (2002) 144–148.
[42] H.M.B. Al-Hashemi, O.S.B. Al-Amoudi, A review on the angle of repose of granular materials, Powder Technol. 330 (2018) 397–417.
[43] ASTM-D6773–-16, Standard Shear Test Method for Bulk Solids Using the Schulze Ring Shear Tester, ASTM International, West Conshohocken, PA, 2008.
[44] G. Félix, V. Falk, U. D'Ortona, Granular flows in a rotating drum: the scaling law between velocity and thickness of the flow, Eur. Phys. J. E 22 (2007) 25–31.
[45] R. Brewster, G.S. Grest, A.J. Levine, Effects of cohesion on the surface angle and velocity profiles of granular material in a rotating drum, Phys. Rev. E 79 (2009), 011305.
[46] P. Garca-Triñanes, S. Luding, H. Shi, Tensile strength of cohesive powders, Adv. Powder Technol. 30 (2019) 2868–2880.
[47] N.-S. Cheng, K. Zhao, Difference between static and dynamic angle of repose of uniform sediment grains, Int. J. Sediment Res. 32 (2017) 149–154.
[48] E. Lajeunesse, A. Mangeney-Castelnau, J. Vilotte, Spreading of a granular mass on a horizontal plane, Phys. Fluids 16 (2004) 2371–2381.
[49] Z. Liu, Measuring the angle of repose of granular systems using hollow cylinders, Ph. D. thesis, University of Pittsburgh, 2011.
[50] H.M. Al-Hashemi, A.H. Bukhary, Correlation between california bearing ratio (cbr) and angle of repose of granular soil, Electron. J. Geotech. Eng. 21 (2016) 5655–5660.